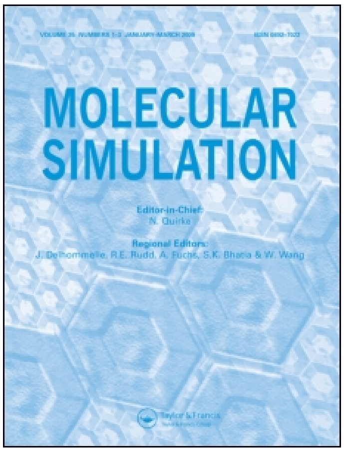

Molecular Simulation

Publication details, including instructions for authors and subscription information:
http://www.informaworld.com/smpp/title~content=t713644482

Model for Molecular Interactions in Helicoidal Cavities

C. Girardet[a]; P. N. M. Hoang[a]; J. Breton[b]
[a] Laboratoire de Physique Moléculaire-URA CNRS 772, Faculté des Sciences-Université de Franche-Comté, Besançon cedex, France [b] Departamento de Fisica Fundamental y, Experimental Universidad de La Laguna, La Laguna-Tenerife, Spain

To cite this Article Girardet, C. , Hoang, P. N. M. and Breton, J.(1996) 'Model for Molecular Interactions in Helicoidal Cavities', Molecular Simulation, 17: 4, 289 — 301

To link to this Article: DOI: 10.1080/08927029608024113

URL: http://dx.doi.org/10.1080/08927029608024113

Molecular Simulation, 1996, Vol. 17, pp. 289–301
Reprints available directly from the publisher
Photocopying permitted by license only

MODEL FOR MOLECULAR INTERACTIONS IN HELICOIDAL CAVITIES

C. GIRARDET[1], P. N. M. HOANG[1] and J. BRETON[2]

[1]*Laboratoire de Physique Moléculaire-URA CNRS 772*
Faculté des Sciences-Université de Franche-Comté-
25030 Besançon cedex-France
[2]*Departamento de Fisica Fundamental y Experimental*
Universidad de La Laguna-38203 La Laguna-Tenerife-Spain

(Received November 1995; accepted April 1996)

A Fourier transform procedure using curvilinear coordinates is developed to determine the interaction potential between a molecule and a helicoidal cavity. When the molecular orientation is free inside the cavity, straightforward criteria for the applicability of the continuum approximation and the molecular confinement along the cavity axis are obtained. At low temperature, the molecule does not rotate freely, being generally trapped in potential wells outside the helix axis and numerical calculations are required to verify whether these criteria hold. An application to N_2 trapped in an $AlPO_4$-5 cavity shows that the molecule center of mass is confined close to the cavity axis with the molecular axis collinear to the cavity axis.

Keywords: Helicoidal cavities; fourier transforms; $AlPO_4$-5

1. INTRODUCTION

Synthetic zeolites and aluminophosphates [1] have gained remarkable interest as adsorbents to study molecular adsorption in porous materials [2]. These molecular sieves are formed by regular pore structures with well-defined shapes and sizes and they can be schematized by using the model of perfect zeolite crystal, for which the positions of the atomic constituents are known. Understanding the adsorption inside pores has been greatly enlightened by a concomitant analysis of data issued from more and more accurate experimental probes including thermodynamics [3–5], spectroscopy [6–7] and diffraction patterns [4,8] and of results of Monte Carlo and molecular dynamics simulation calculations [9–14].

The accuracy of the theoretical methods rests on the knowledge of the interaction potential between the adsorbate and the adsorbent and, when the potential is known, on the adequacy of the analytical or numerical expressions regarding the computational technique. Simple potential forms and sum truncations over the spatial atomic arrangement in zeolite are generally required to save computing time. These two approximations can yet provide inaccuracies. Therefore all the potential calculations are performed by considering the competition between a minimum computational time and an optimum accuracy. While pairwise atom-atom or site-site additive potentials seem to be rather appropriate for simulations, they remain time consuming and the continuum approximation [15] appears to be an efficient but sometimes questionable way of obtaining fast results on the adsorption properties of various molecules. The question is thus open in order to determine the criteria which make valid the continuum approximation when compared to an exact numerical calculation.

In previous papers [16–18], we considered the interaction between a confined atom and a helicoidal cavity which schematizes the local distribution of oxygen atoms in a pore of an aluminophosphate compound. The potential periodicity connected to the spatial arrangement of the oxygen atoms along coaxial helices was used to perform a Fourier transform analysis of the atom-helix interaction. Here, we extend the method to the interaction between a molecule and a helix and consider the molecule as a set of atom sites characterized by dispersion-repulsion parameters. The geometry of the system is described in Sec. 2 for the case of a diatomic molecule inside the helicoidal cavity. The Fourier analysis is then performed in Sec. 3. Implications on molecular confinement for very simple situations are discussed in Sec. 4, with an illustration to the adsorption of N_2 inside a $AlPO_4$-5 micropore.

2. GEOMETRY OF THE SYSTEM

Let us consider a periodic arrangement of atoms along a helix defined by its radius ρ and its pitch B. N is the atom number per helix pitch along the curvilinear coordinate t. The position of a generical helix atom is defined with respect to the absolute frame $(\vec{X}, \vec{Y}, \vec{Z})$ ($\vec{Z}$ along the helix axis) by its components $(\rho\cos 2\pi\eta t;\ \rho\sin 2\pi\eta t;\ B\eta t)$, where η characterizes the inverse of the length of the helix pitch

$$\eta^{-1} = ((2\pi\rho)^2 + B^2)^{1/2} = NS_h \tag{1}$$

S_h is the distance between consecutive atoms along the helix curvilinear coordinate. The length of the primitive vector in the reciprocal space is written as

$$G_g = 2\pi g / S_h; \quad g \text{ integer} \tag{2}$$

The position $\vec{R}$ of the molecule center of mass is defined by its components (X, Y, Z) in the absolute frame while the absolute position $\vec{R}_i$ of the ith constituent in the probe molecule is expressed as

$$\vec{R}_i = \vec{R} + \vec{r}_i(\vec{\Omega}) \tag{3}$$

where $\vec{r}_i$ depends on the internal molecular geometry and on the orientational degrees of freedom $\vec{\Omega}$. The coordinates (X_i, Y_i, Z_i) of the ith atom are expressed in terms of the curvilinear coordinate S_i which defines the intersect C_i of the helix with the plane perpendicular to the helix axis and containing the ith atom (Fig. 1). Let $\vec{\xi}_i$ be the vector joining C_i to the position of the ith atom center of mass, the absolute coordinates of this atom are written as

$$\begin{aligned} X_i &= (\rho + \xi_{x_i}) \cos 2\pi\eta S_i - \xi_{y_i} \sin 2\pi\eta S_i \\ Y_i &= (\rho + \xi_{x_i}) \sin 2\pi\eta S_i + \xi_{y_i} \cos 2\pi\eta S_i \\ Z_i &= B\eta S_i \end{aligned} \tag{4}$$

The distance between the ith atom in the probe molecule and the generical atom in the helix is given in the more general way, as

$$\begin{aligned} d_i^2(S_i - t, \vec{\xi}_i) = {} & (\xi_{x_i} + \rho(1 - \cos 2\pi\eta(S_i - t)))^2 + (\xi_{y_i} + \rho \sin 2\pi\eta(S_i - t))^2 \\ & + (B\eta(S_i - t))^2 \end{aligned} \tag{5}$$

While it appears judicious to keep the variables S_i and $\vec{\xi}_i$ to perform the Fourier analysis of the potential, it must be recalled that this set of variables depends on the molecule geometry, *i.e.* the internal configuration of the atoms in the molecule and the external coordinates of the molecule. It is interesting to make explicit such a dependence for the case of the diatomic molecule. Let $\vec{\xi}$ be the center of mass position with respect to C (Fig. 1) characterized by its curvilinear coordinates, S, $\vec{\Omega}(\theta, \varphi)$ the angles defining the axis orientation of the molecule and r_i the distance of the ith atom with

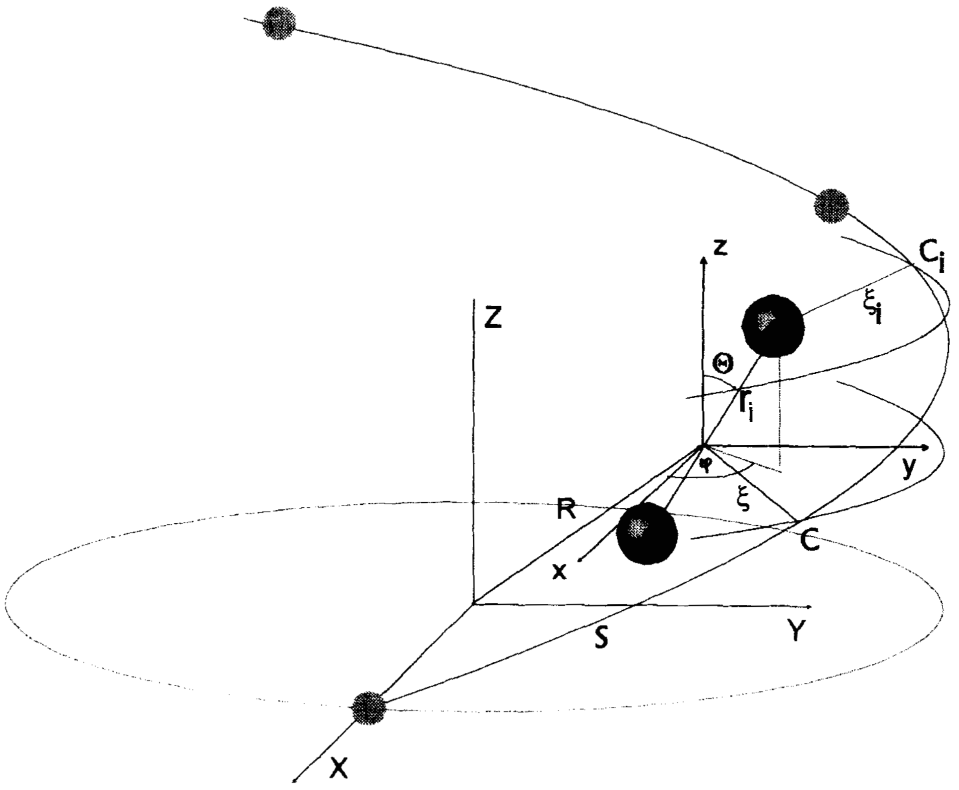

FIGURE 1 Geometry of the helix-diatomic molecule system; $\vec{R}$ and $\vec{\Omega}$ define the molecular center of mass position and axis orientation in the absolute frame $(\vec{X},\vec{Y},\vec{Z})$. The points C_i and C characterize the intersect of the helix with $(\vec{X},\vec{Y})$ planes containing the ith atom and the molecular center of mass, respectively.

respect to the molecule center of mass, the change of atomic to molecular variables is expressed as

$$S_i = S + \frac{r_i}{B\eta}\cos\theta$$

$$\xi_{x_i} = \xi_x + r_i \sin\theta\cos(2\pi\eta S - \varphi) + \rho\left(\cos 2\pi\eta S - \cos 2\pi\left(\eta S + \frac{r_i}{B}\cos\theta\right)\right) \quad (6)$$

$$\xi_{y_i} = \xi_y - r_i \sin\theta\sin(2\pi\eta S - \varphi) + \rho\left(\sin 2\pi\eta S - \sin 2\pi\left(\eta S + \frac{r_i}{B}\cos\theta\right)\right)$$

Using Equation (6), the distance d_i given by Equation (5) is thus transformed into an expression $d_i^2(S-t, S, \vec{\Omega}, r_i)$ which depends on the relative curvilinear coordinate S-t and on the molecular characteristics $(S,\vec{\Omega},r_i)$. The expression of d_i^2 becomes much simpler when the molecular center of mass is located along the helix axis $(\vec{\xi} = -\vec{\rho})$, leading to

$$d_i^2(u_i) = u_i^2 + a_i^2 - 2b_i \cos\left(\alpha_i + \frac{2\pi}{B} u_i\right) \tag{7}$$

where a_i, b_i and α_i depend on the helix radius and on the molecular characteristics $(r_i,S,\vec{\Omega})$

$$\begin{aligned} a_i^2 &= \rho^2 + r_i^2 \sin^2\theta \\ b_i &= \rho r_i \sin\theta \\ \alpha_i &= \varphi - 2\pi\left(\eta S - \frac{r_i}{B}\cos\theta\right) \end{aligned} \tag{8}$$

and $u_i = B\eta(S-t) + r_i \cos\theta$ defines the new variable.

3. FOURIER ANALYSIS OF THE POTENTIAL

3.1. General Expression

The interaction potential between a molecule and a neutral helix atom is obtained as a sum of dispersion-repulsion contribution. Here we consider the simple situation for which the dispersion-repulsion is described by an atom-atom Lennard-Jones form. Simulation calculations generally use this type of interactions in zeolites. The potential between the *i*th atom in the molecule and the *k*th helix atom is given as

$$V_{ik} = \sum_{n=6,12} \frac{(-)^{n/2} C_n^{ik}}{d_i^n(S_i - t, \vec{\xi}_i)} \tag{9}$$

C_n^{ik} is the potential parameter equal to C_6 or C_{12} for the dispersion and repulsion terms and the distance d_i is given by Equation (5).

The Fourier expansion of the potential [16], after summing over the atoms of the probe molecule and over the atom distribution along the helix, assumed to be infinitely long, leads to

$$V(S,\vec{\xi},\vec{\Omega},r_i)=\sum_i W_{i,o}+2\sum_i\sum_{g>0}\left\{W^R_{i,g}\cos 2\pi g\eta\left(S+\frac{r_i}{B\eta}\cos\theta\right)\right.$$

$$\left.+W^I_{i,g}\sin 2\pi g\eta\left(S+\frac{r_i}{B\eta}\cos\theta\right)\right\}$$

where the Fourier coefficients are given by (R and I correspond to cosine and sine terms, respectively)

$$W^{R,I}_{i,g}=\sum_{n=6,12}N\eta\int_{-\infty}^{+\infty}dt\mathop{}^{\cos}_{\sin}\left[2\pi gN\eta(S-t+\frac{r_i}{B\eta}\cos\theta)\right]\frac{(-)^{n/2}C^{ik}_n}{d^n_i(S_i-t,\vec{\xi}_i)}\tag{11}$$

The analytic calculation of these coefficients is possible for special configurations of the probe molecule. Otherwise, a numerical computation of Equation (11) is required. Thus, when the molecular center of mass is along the helix axis, the Fourier coefficients become

$$W_{i,o}=\sum_{n=6,12}\frac{N}{B}\int_{-\infty}^{+\infty}du_i\frac{(-)^{n/2}C^{ik}_n}{\left[u_i^2+a_i^2-2b_i\cos\left(\alpha_i+\frac{2\pi}{B}u_i\right)\right]^{n/2}}\tag{12}$$

$$W^{R,I}_{i,g}=\sum_{n=6,12}\frac{N}{B}\int_{-\infty}^{+\infty}du_i\mathop{}^{\cos}_{\sin}\left[2\pi g\frac{N}{B}u_i\right]\frac{(-)^{n/2}C^{ik}_n}{\left[u_i^2+a_i^2-2b_i\cos\left(\alpha_i+\frac{2\pi}{B}u_i\right)\right]^{n/2}}$$

These expressions reduce to simple known integrals when the molecular axis is furthermore oriented along the helix axis ($\theta=0$ or $\pi; a_i=\rho; b_i=0$) and the calculation of the Fourier coefficients (performed as explained in Reference [16]) leads to an analytical expression for the molecule-helix interaction potential

$$V(Z,r_i)=\frac{8\pi}{3}\frac{N}{B}\left(-\rho^{-5}\sum_{i=1}^{2}C^{ik}_6+\frac{21}{32}\rho^{-11}\sum_{i=1}^{2}C^{ik}_{12}\right)$$

$$+\frac{\pi}{8}\frac{N}{B}\sum_{g>0}\sum_{i=1}^{2}e^{-2\pi g\rho N/B}\cos\left[2\pi gN(Z+(-)^{i-1}r_i)/B\right]\tag{13}$$

$$\times(\rho^{-5}S_6(4\pi g\rho N/B)C^{ik}_6-(\rho^{-11}/64)S_{12}(4\pi g\rho N/B)C^{ik}_{12})$$

where the function $S_n(x)$ is defined in Reference [16]. The potential V depends on the internal molecular coordinates $r_i (i = 1$ and $2)$ and on the position Z of the molecular center of mass along the axis through the cosine term, only. The zero order Fourier coefficient is obviously independent of Z and it depends on the molecular characteristics through the sum of the Lennard-Jones coefficients of each atom. The convergence of the Fourier expansion is characterized by the decrease of the product of the exponential term and the S_n function, while the magnitude of the potential is modulated by the cosine, thus reflecting the cavity corrugation experienced by the molecule along the equilibrium valley.

3.2. Average Potential

A general analysis of the convergence of the Fourier transform procedure is very difficult since it depends on the position and orientation of the molecule inside the helix. Therefore we rather consider the mean potential experienced by the molecule which is defined as the average over the free rotation of the molecule in the cavity. Let $\bar{V}_k$ be this mean potential between the ith atom in the molecule and the kth helix atom

$$\bar{V}_k = \frac{1}{4\pi} \int \sum_{i=1}^{2} v_{ik} \sin\alpha \, d\alpha \, d\beta \tag{14}$$

where α and β characterize the angles of the molecular axis with respect to a frame tied to the molecule-kth helix atom pair. The dispersion-repulsion potential for the molecule-kth helix atom pair can be written as

$$\bar{V}_k = \sum_{n=6,12} (-)^{n/2} \frac{\sum_{i=1}^{2} \bar{C}_n^{ik}(r_i, d)}{d^n(S - t, \vec{\xi})} \tag{15}$$

where now the distance d characterizes the molecular center of mass position with respect to the generical helix atom; d is obtained from Equation (5) by changing $\vec{\xi}_i$ into $\vec{\xi}$ and S_i into S. The Lennard-Jones parameters $\bar{C}_n^{ik}$ depend on the distance d and on the internal characteristics of the molecule through r_i (cf. Appendix A). Assuming that these parameters are effective and disregarding their d dependence leads to an expression for the molecule-helix interaction potential identical to that calculated [16] for an effective atom interacting with the helix, since all the orientational dependence disappears after averaging.

4. DISCUSSION

Two characteristics for the molecular adsorption in a helicoidal cavity are discussed here, regarding on one hand the convergence of the Fourier expansion and the validity of the continuum approximation and, on the other hand the condition for the molecule confinement along the helix axis. We consider reduced variables for the mean potential and define $\rho^* = \rho/\bar{\sigma}$, $B^* = B/\bar{\sigma}$, $b^* = B/N\bar{\sigma}$ and $\bar{V}^* = \bar{V}/\bar{\varepsilon}$ where $\bar{\varepsilon}$ and $\bar{\sigma}$ are the effective Lennard-Jones parameters for the average molecule-helix atom pair.

The conditions for the applicability of the continuum approximation to the mean interaction potential $\bar{V}^*$, i.e. by retaining only the $g=0$ term in the Fourier expansion, mainly depend on the reduced parameter b^*. The convergence of the Fourier transform procedure is faster when B decreases and/or N increases. This can be interpreted as the result of a higher atomic density along the helix which thus favors the convergence and allows us to limit the g expansion to the first term. Indeed $B/(N\bar{\sigma})$ represents the periodic arrangement of the helix atoms, projected on the helix axis, as viewed by the effective confined molecule. When $b^* \leqslant 0.7$, the continuum approximation holds since the $g=0$ Fourier coefficient reproduces the mean interaction potential map with an accuracy better than 1%. For increasing values of b^* ($0.7 \leqslant b^* \leqslant 1.3$) it is necessary to include the $g=1$ term, while for larger b^* values, the continuum approximation totally fails and higher order terms must be considered. These results are quite consistent with those obtained [17] for the interaction between an atom and a helicoidal cavity, since the single change is the consideration of an effective molecular diameter for the average molecule-helix interaction.

For this freely rotating (average) molecule, the confinement criteria [17] along the helix axis depends mainly on the reduced helix radius ρ^* which accounts for the relative size of the helix cavity and of the average molecule. When $\rho^* \leqslant 1.2$, the center of mass of the average molecule is found to be on the helix axis whatever the values of b^*, whereas for larger values $\rho^* > 1.2$, the equilibrium site for the molecule is outside this axis. As a consequence, the analytic expression of the potential can be used with a fair accuracy when the average size of the molecule is large enough when compared to the cavity size. ($0.8\rho < \sigma < \rho$).

A different behavior is expected for this molecule without averaging over the free rotation, since the failure of spherical symmetry tends to favor special orientations for the molecular axis outside the helix axis. Therefore, the anisotropic molecule can be much more trapped in helix potential wells than the mean molecule, thus requiring a complete calculation of the potential map $V(X, Y, Z, \vec{\Omega})$ in order to verify whether the continuum approximation and the confinement condition hold in that case. As an example we consider the situation of a N_2 molecule trapped in $AlPO_4$-5 micropore [18].

4.1. Application to N_2 adsorbed inside an $AlPO_4$-5 cavity

In the $AlPO_4$-5 micropore, the oxygen atoms forming the internal wall of the cavity are distributed [18] along two sets of coaxial helices with the same radius $\rho = 3.8$ Å and pitch $B = 46.5$ Å. The first set contains six helices with 24 oxygen atoms per pitch while the second set contains six helices with 12 oxygen atoms per pitch. The N_2 probe molecule is described within the two situations, either with a linear shape (low temperature case) or with a spherical (free orientational average) shape (high temperature case). The potential parameters for the oxygen-N_2 pairs are given in Appendix A.

We calculate the interaction potential for the system in the two situations and determine the corresponding equilibrium configuration for the molecule in the cavity. In Figure 2, we show the behavior of the reduced position Δ^* of the molecular center of mass with respect to the cavity axis as a function of the relative radius of the helicoidal cavity for the assumed spherical molecular shape. The curve of values of the minimum potential energy $V_m^*(\rho^*)$ is also drawn. The values of Δ^* monotonically decrease with ρ^* down to $\rho^* \approx 1.25$. Below this value, the center of mass of the molecule moves towards the helix axis with a dramatic change of the curve slope. For $\rho^* \leqslant 1.23$, the molecule is totally confined on the cavity symmetry axis, as already mentioned from general considerations, and the potential is minimum since the molecule ≪sees≫a maximum number of surrounding oxygen atoms. The potential monotonically decreases with ρ^* and it can be analytically determined from the Fourier transform procedure yielding a straightforward expression. At higher values of ρ^* the molecule moves toward the cavity wall and thus ≪sees≫ less oxygen atoms leading to an increase of V_m^*. Moreover, the continuum approximation is quite good for this cavity species since the high oxygen density on the helices leads to b^* values equal to 0.67 and 1.34, depending on the helix set.

We now consider the case of the linear molecule and calculate the equilibrium position and orientation for N_2 in the micropore by minimizing the interaction potential. We find that the molecular center of mass is shifted by 0.57 Å with respect to the cavity axis, and by 1.22 Å (with a periodicity equal to $B/12 = 3.87$ Å) along this axis. The molecular axis is collinear to

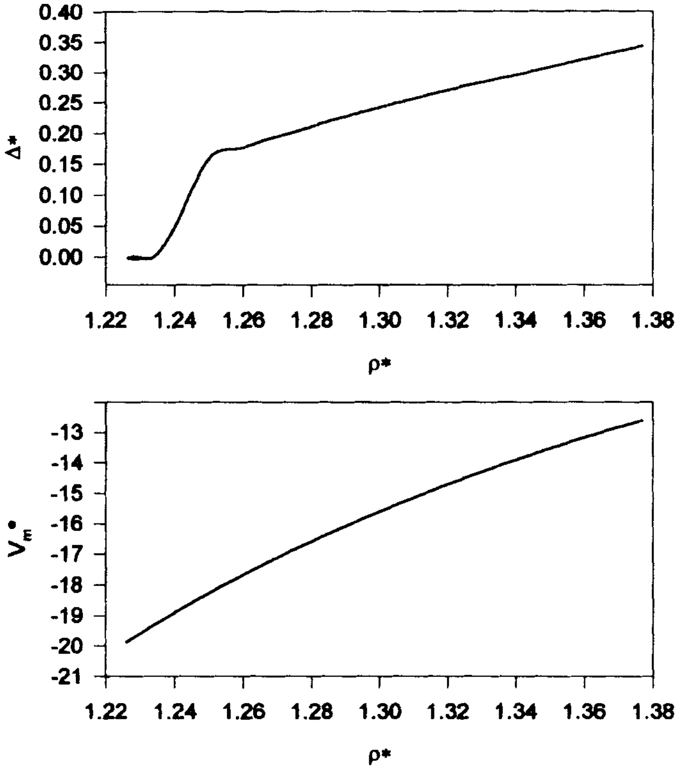

FIGURE 2 (a) Behavior of the reduced molecular position Δ^* for the average N_2 molecule with respect to the cavity axis as a function of the reduced radius ρ^* of the $AlPO_4$-5 cavity; (b) corresponding behavior of the reduced potential vs. ρ^*.

the cavity axis ($\theta = 0$) and the corresponding value of the potential is -134 meV. This latter result agrees with the data [3–5] of isosteric heat of adsorption (-144 meV) and considerably improves the value determined [18] for the spherical molecule (-86 meV). From these results, we see that $\rho^* \approx 1.27$ for the linear N_2 molecule while $\rho^* \approx 1.23$ for the spherical shape, and that the confinement criterium holds approximately, only. Therefore the analytical potential expression given in Equation (13) is reasonably accurate and it yields maximum and minimum values depending on the cosine term. For $g = 1$, the cosine term is minimum for $Z = (b^* \bar{\sigma} \pm r)/2$ yielding an equilibrium value for Z around 1.1 Å, in agreement with the exact calculations.

Our conclusion is that the trapping of N_2 in the $AlPO_4$-5 micropore can be accurately described within the continuum approximation or, better, within an improved expansion of the Fourier transform procedure limited to the first two terms ($g = 0$ and 1). However the fact that the N_2 center of mass is not strictly confined along the axis, requires a calculation of the potential which goes beyond the simple expression given by (Eq. 13). Indeed, this latter equation yields only a potential estimate which is reflected by the monotonic increase of the spherical potential with ρ^* since the corresponding potential value is -115 meV, *i.e.* underestimated by about 14%. A more general study of this convergence criterium should be extended to other probe molecules in zeolite, including other potential contributions. Nevertheless, it seems that this Fourier analysis procedure is an efficient way of performing fast potential calculations which are used as intermediate data for involved simulations on dynamical and kinetical properties of adsorbates in porous materials.

Acknowledgements

One of us (J. B.) would like to thank the Consejeria de Education del Gobierno Autonomo de Canarias for a financial support of this work (PI 077/92).

APPENDIX

Effective Lennard-Jones parameters

The average over the molecule orientation leads to $\bar{C}_n^{ik}$ terms defined as

$$\bar{C}_6^{ik}(d,r_i) = C_6^{ik}\frac{1 + r_i^2/d^2}{(1 - r_i^2/d^2)^4}$$

$$\bar{C}_{12}^{ik}(d,r_i) = C_{12}^{ik}\frac{1 - 12r_i^2/d^2 + 25.2r_i^4/d^4 + 12r_i^6/d^6 + r_i^8/d^8}{(1 - r_i^2/d^2)^{10}} \tag{A1}$$

These parameters are nearly d independent for $r_i/d \ll 1$. When the molecular center of mass is located along the helix axis $d \equiv \rho$, the accuracy varies as $(r_i/\rho)^2$ which in general remains small (a few percent). The effective parameters for the average molecule are then given as

$$\bar{C}_6 \simeq \sum_{i=1}^{2} \bar{C}_6^{ik}(\rho,r_i) = 4\bar{\varepsilon}\bar{\sigma}^6$$

$$\bar{C}_{12} \simeq \sum_{i=1}^{2} \bar{C}_{12}^{ik}(\rho,r_i) = 4\bar{\varepsilon}\bar{\sigma}^{12} \tag{A2}$$

The values of the parameters are [17]:
$\bar{\varepsilon}_{N_2\text{-}O} = 5.9$ meV, $\bar{\sigma}_{N_2\text{-}O} = 3.10$ Å for the average molecule; $\varepsilon_{N\text{-}O} = 3.9$ meV, $\sigma_{N\text{-}O} = 2.99$ Å for the atom-atom pair.

References

[1] Smith, J. V. (1988) "Topochemistry of Zeolites and Related Materials. 1. Topology and Geometry" *Chem. Rev.*, **88**, 149.

[2] Furuyama, S., Miyazaki, M. and Inoue, H., (1984) "Sorption of Argon, Oxygen, Nitrogen, Nitric Oxide, and Carbon Monoxide by Hydrogen Mordenite, Hydrogen ZSM-5 Synthetic Zeolite, and Sodium Hydrogen Mordenites" *J. Phys. Chem.*, **88**, 1741. Feller, U. M., Reichert, H., Kokotailo, G. T., Unger, K. K., Grillet, Y., Rouquerol, F. and Rouquerol, J. "High Resolution Nitrogen and Argon Sorption Studies: Properties of Microporous MFI-Type Network Zeolites Compared to AFI- and AEL-Type Aluminophosphate Molecular Sieves." Proceeding IIIrd Int. Conf. on Fundamentals of Adsorption (1991) 595.

[3] Reichert, H., Muller, U., Unger, K. K., Grillet, Y., Roquerol, F., Rouquerol J. and Coulomb, J. P. (1991) "Sorption of argon and nitrogen on network types of zeolites and aluminophosphates" in Characterization of Porous Solids II, Rodriguez-Reinoso Ed. (Elsevier, Amsterdam), 535.

[4] Llewellyn, P. L., Coulomb, J. P., Grillet, Patarin, J., Lauter, H., Reichert H. and Rouquerol, J. (1993) "Adsorption by MFI-Type Zeolites Examined by Isothermal Microcalorimetry and Neutron Diffraction. 1. Argon, Krypton, and Methane" Llewellyn, P. L., Coulomb, J. P., Grillet, Y., Patarin, J., Lauter, H., Reichert, H. and Rouquerol, J. "Adsorption by MFI-Type Zeolites Examined by Isothermal Microcalorimetry and Neutron Diffraction. 1. Nitrogen and Carbon Monoxide", *Langmuir*, **9**, 1852.

[5] Tosi-Pellenc, N., Grillet, Y., Rouquerol, J. and Llewellyn, P. (1992) "A Microcalorimetric comparison of the adsorption of various gases on two microporous adsorbents: a model of aluminophosphate and a natural clay" *Thermochim. Acta.*, **204**, 79.

[6] Cohen de Lara, E. R. (1989) "Experimental and theoretical determination of vibrational frequency shifts of diatomic molecules adsorbed in NaA zeolite. Interaction potential and its derivatives with respect to the internal coordinate of H_2, D_2, N_2, O_2." *Mol. Phys.*, **66**, 479; Jameson, C. J., Jameson, A. K., Gerald, R., II and De Dios, A. C. (1992) "Nuclear magnetic resonance studies of xenon clusters in zeolite NaA" *J. Chem. Phys.*, **96**, 1676.

[7] Furuki, M., Kubota, J., Goto, Y., Wakabayashi, F., Kondo, J. Wada, A. Domen, K. and Hirose, C. (1993) "Vibrational lifetime of surface species of zeolites by picosecond IR pulses" *J. Elect. Spect. and Rel. Phenom.*, **64/65**, 259.

[8] Fang M. P., Sokol P. E. and Wang, Y. (1994) "Structure of D_2 in zeolite" *Phys. Rev.*, **B 50**, 12291.

[9] Panagiotopoulos, A. Z. (1987) "Adsorption and capillarity condensation of fluids in cylindrical pores by Monte Carlo simulation in the Gibbs ensemble" *Mol. Phys.*, **62**, 701.

[10] Soto J. L. and Myers, A. L. (1981) "Monte Carlo Studies of Adsorption in Molecular Sieves" *Mol. Phys.*, **42**, 971; Woods, G. B. Panagiotopoulos A. E. and Rowlinson, J. S. (1988) "Adsorption of Fluids in Model Zeolite Cavities" *Mol. Phys.*, **63**, 49; Smit B. and Den Ouden, C. J. J. (1988) "Monte Carlo Simulations on the Relation between the Structure and Properties of Zeolites: The Adsorption of Small Hydrocarbons" *J. Phys. Chem.*, **92**, 7169.

[11] Cracknell R. F. and Gubbins, K. E. (1993) "Molecular Simulation of the Adsorption and Diffusion in VPI-5 and Other Aluminophosphates" *Langmuir*, 9, 824.

[12] Razmus, D. M. and Hall, C. K. (1991) "Prediction of Gas Adsorption in 5A Zeolites Using Monte Carlo Simulation" *Alche Journal*, **37**, 769.

[13] Boutin, A., Pellenq, R. J. M. and Nicholson, D. (1994) "Molecular simulation of the stepped adsorption isotherm of methane in AlP04-5", *Chem. Phys. Lett.*, **219**, 484.

[14] Nivarthi, S. S., Van Tassel, P. R. Davis, H. T. and Mc Cormick, A. V. (1995) "Adsorption and energetics of Xenon in mordenite: A Monte Carlo simulation study" *J. Chem. Phys.*, **103**, 3029.

[15] Baksh, M. S. A. and Yang, R. T. (1991) "Model for Spherical Cavity Radii and Potential Functions of Sorbates in Zeolites", *Alche Journal*, **37**, 923.

[16] Alvira, E., Breton, J., Delgado, V. and Girardet, C. (1992) "Interaction Between an Atom and a Mesoscopic Helicoidal System -Fourier Transform Analysis" *J. Chem. Phys.*, **97**, 6821.

[17] Gonzales-Platas, J. Breton, J. and Girardet, C. (1993) "Atom Confinement in Helicoidal Cavities" *J. Chem. Phys.*, **98**, 3389.

[18] Gonzales-Platas, J. Breton, J. and Girardet, C. (1995) "Physisorption in a Molecular Helicoidal Cavity: Application to AlP04-5" *Langmuir*, **11**, 197.